

R. Subedi,¹ X. Deng,² D. Wang,² R. Michaels,³ P. Jenner,⁴ and X. Zheng²

¹George Washington University, 725 21st St, NW, Washington, DC 20052, USA

²University of Virginia, Charlottesville, Virginia 22904, USA

³Thomas Jefferson National Accelerator Facility, Newport News, Virginia 23606, USA

⁴Argonne National Laboratory, Argonne, Illinois, 60439, USA

(Dated: April 27, 2010)

Parity violating deep inelastic scattering experiment in Hall A at Thomas Jefferson National Accelerator Facility (Jefferson Lab) has a goal of measuring a combination of the axial hadronic couplings of the electron with a factor of six improvement in precision over world data. Precise data for the couplings are essential to search for physics beyond the Standard Model. The experiment has measured a 10^{-4} level asymmetry using polarized electron scattering from deuterium with a beam energy of 6 GeV. A highly specialized data acquisition (DAQ) system with inherent particle identification was developed and utilized. The DAQ of this experiment is discussed with an emphasis on the capability of measuring deadtime, pileup effects, and small asymmetry.

PACS numbers: 21.10.Hw, 25.30.-c

Introduction

Parity violating deep inelastic scattering (PVDIS) experiment E08-011 completed its data taking in the end of 2009. The goal of this experiment [1–3] is to measure precisely the asymmetry in parity violating deep inelastic scattering of a polarized electron on an unpolarized liquid deuterium target. This asymmetry is sensitive to the effective vector electron axial quark and axial electron vector quark couplings, the former of which is extremely poorly constrained by experimental data.

The electromagnetic interaction is parity conserving as it is insensitive to the spin flip of the incoming electron beam. Only the weak interaction violates parity. Taking the difference of the left-handed and right-handed electron scattering cross-sections, one can isolate the parity violating contribution of the weak interactions. That means, if we measure the two mirror-image scattering

processes in the same experimental conditions, the difference between the two counting rates can isolate the weak contribution due to the Z-boson exchange. With σ_+ and σ_- as the left-handed and right-handed electron cross-sections, respectively, and Q^2 as the negative of the square of the four-momentum transfer, the parity violating asymmetry, A_{pv} , that can be measured experimentally, is given as

$$A_{pv} = \frac{\sigma_+ - \sigma_-}{\sigma_+ + \sigma_-} \cong Q^2 [100 \text{ ppm/GeV}^2].$$

The theoretical expression for such an asymmetry is given by equation (1). Here G_F is the Fermi weak coupling constant, α is the fine structure constant, Y is a kinematic factor, R_s and R_v are sea- and valence-quark distribution functions, C_{iq} are effective coupling constants, and x is the Bjorken variable (see for details in ref. [1]).

$$A_{PV} = \left(\frac{3G_F Q^2}{\pi\alpha^2 \sqrt{2}} \right) \frac{2C_{1u}[1 + R_C(x)] - C_{1d}[1 + R_S(x)] + Y(2C_{2u} - C_{2d})R_V(x)}{5 + R_S(x) + 4R_C(x)}. \quad (1)$$

Taking effective coupling constants C_{iq} in the context of the Standard Model as

$$C_{1u} = g_a^e g_v^u = -\frac{1}{2} + \frac{3}{4} \sin^2(\theta_w),$$

$$C_{2u} = g_v^e g_a^u = -\frac{1}{2} + 2 \sin^2(\theta_w),$$

$$C_{1d} = g_a^e g_v^d = \frac{1}{2} - \frac{2}{3} \sin^2(\theta_w),$$

$$C_{2d} = g_v^e g_a^d = \frac{1}{2} - 2 \sin^2(\theta_w)$$

this experiment will extract an effective coupling con-

stant combination $(2C_{2u} - C_{2d})$ with a high precision. There are two Q^2 data points taken in this experiment so as to extract the experimental result for the hadronic correction, $c(x)$, due to higher-twist (HT) effects

$$A_{pv}(x, Q^2) = A_{pv}(x)(1 + c(x)/Q^2),$$

whose value is believed to be impossible to get from the first principles [4]. The plan was to find asymmetry at low Q^2 point and extract HT there. Next, use that HT while measuring asymmetry at the high Q^2 point.

The experiment was performed in Hall A using two

standard spectrometer setups [5] at two Q^2 points: the first Q^2 point being 1.1 (GeV/c)^2 with incident electron energy $E = 6.0 \text{ GeV}$, scattered electron energy $E' = 3.66 \text{ GeV}$, Bjorken $x = 0.25$, and scattered electron angle $\theta = 12.9^\circ$, and the second Q^2 point being 1.9 (GeV/c)^2 with $E = 6.0 \text{ GeV}$, $E' = 2.63 \text{ GeV}$, $x = 0.30$, and $\theta = 20.0^\circ$. The both Q^2 points used about 89% polarized electron beam of $100 \mu\text{A}$ on a 20 cm long deuterium target.

Data Acquisition System

The combination of preshower and shower detectors was the main detector for the PVDIS experiment. This experiment was expecting a high event rate of about 0.5 MHz from the main detector in each spectrometer. The conventional DAQ could handle only up to a 4 kHz of event rate and it was inapplicable for this experiment. Hence there was an immense need of developing a new DAQ to run the PVDIS experiment. As a result, the new DAQ developed for (and used by) this experiment had a unique counting DAQ that employed a hardware based particle identification (PID). This was necessary for separating a large pion background from the electron signal. The integrating DAQ used by previous parity violating experiments at Jefferson Lab could not be adopted here as the integrating DAQ had no mechanism to reject the pion background.

The electron and pion signals were obtained through different routes in the DAQ (see Fig. 1). They went through both narrow and wide paths. These two paths were designed to study deadtime effects. The main component of the counting DAQ was a scaler module. The scaler counting is always deadtimeless. The high rate digital signal fed into the scaler module would give the final readout of the PVDIS data.

There was a big effort to decide whether to use overlapping or non-overlapping scheme in achieving a high signal detection efficiency from the main detector, specially in the region where two adjacent blocks share the same signal. We found that there was no gain in efficiency using the overlapping scheme over the non-overlapping one. This was confirmed by a simulation using real data input. This led us to choose the non-overlapping scheme which saved us a significant amount of electronics modules along with a possible loss of man-power in debugging the extra electronics in the DAQ, had we used the overlapping scheme. The electron PID efficiency obtained using the non-overlapping scheme, such as shown in Fig. 2, was found to be already about a cent percent; the choice of the non-overlapping scheme had a merit.

The shower detector in right high resolution spectrometer (rhhs) had 64 lead blocks with a photo-multiplier tube (PMT) attached in one end only, giving a 64 output channels. The preshower detectors in the both high

resolution spectrometers had 48 output channels coming from 48 bars, with a PMT in one end in each bar again. The preshower blocks were stacked with a row of two bars where the end of the bars that did not have PMTs faced each other. All preshower blocks were individually wrapped to block light leak. The preshower detector signal from each PMT in the rhhs had to be split into two using a passive splitter in order to produce the same number of output channels as that in the shower detector. Since only the 64 channels out of 96 available preshower channels after splitting had to be used, the unused preshower signals were terminated by a 50Ω terminator. In the left high resolution spectrometer (lhhs), both preshower and shower detectors had a similar construction, there was no need to split any signal, as the number of detector channels in the both were the same.

The detector signals (a detector means a shower or a preshower detector in this context), in a group of 8 channels, were directly input to a linear summing module called SUM8 (represented by SS or PS with a different indexing in the DAQ flowchart: Fig 1). The preshower signal splitting was performed before this stage. The SUM8 module had two applications: summing all the input signals to produce a single output, and fanning out each input signal to yield its identical copy for an elsewhere use. We used all the fan-out copies to a regular spectrometer DAQ so as to get information for tracking, with or without the use of VDCs (vertical drift chambers), carrying out a regular spectrometer DAQ running. After SUM8, there was another stage of linear summing (represented by TS with a different indexing in the DAQ flowchart: Fig 1) where we combined the shower and preshower signals. A random high rate signal, called tagger, did also enter here. Some of these linear summing modules also combined the tagger with a preshower signal only. The analog signal after this linear summing was digitized using a leading edge discriminator. After digitization, the signal was driven through different logic modules and finally taken to a NIM to ECL module to produce outputs in ribbon cables so as to route the signal to a scaler module as a final destination. Any signal that went to a scaler module of the counting DAQ also went to a TDC module in a regular spectrometer DAQ. The TDC module signals were used to time-align all the detector signals. This alignment in time was performed before going to the production mode of data taking.

Two types of veto signals were prepared using a combination of scintillator and gas-cherenkov triggers: electron veto and pion veto. The scintillator trigger came from two layers of scintillator paddles that were normally used to provide the main trigger for the regular spectrometer DAQ [5]. The purpose of such veto triggers was to give a clean PID for electron and pion triggers. Referring to the DAQ flowchart diagram (Fig 1), the logic modules that had veto signal input would only give outputs if and only if the veto signal was present.

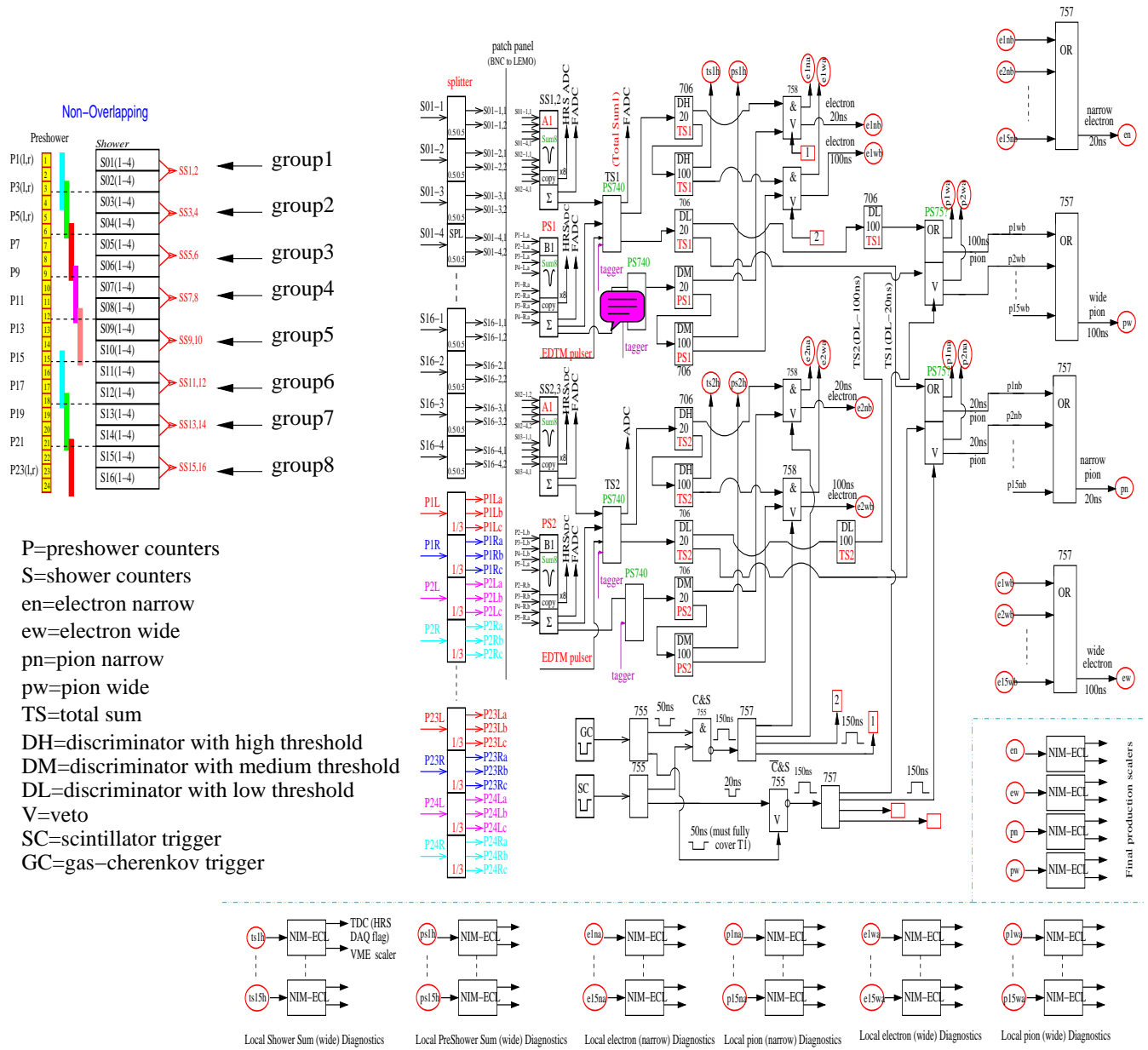


FIG. 1: A typical DAQ flowchart diagram showing eight groups in the front, and two groups in action afterward, using a non-overlapping DAQ scheme. This diagram represents the exact form of the flowchart as used in the rhrs. For the case of lhrs, there was a slight modification, since the shower and preshower detectors in the lhrs had the same construction, unlike that in the rhrs. Regarding groupings, we had eight groups in rhrs and six groups in lhrs. The difference in the total group number is due to the fact that the two spectrometers had different type of shower detector construction, though the two spectrometers had a similar type of preshower detectors. In the case of shower detectors, the left hrs had its shower detector similar to its preshower detector in terms of detector numbers, whereas the rhrs had 80 shower blocks with one PMT in end only (see ref [5] for details) although we used only 64 of them only. The non-overlapping scheme is shown on the top left: one group has 8 PMT channels, 4 preshower bars form a group; the color coded vertical bars beside the preshower stack represent a group in the preshower stack. In the rhrs shower detector, two rows form a group, each row has four PMT channels.

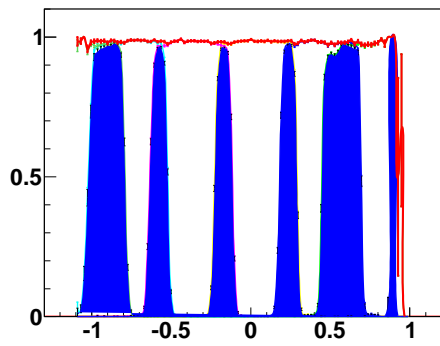


FIG. 2: Red trace shows PID efficiency for electrons and it is almost 100%. Horizontal axis is the two meter long coverage of the main detector on the dispersive direction. Blue shading is the double counting in efficiency in two adjacent groups, this double counting is carefully excluded in the red trace. Though this plot belongs to electron PID efficiency in the left hrs through a narrow path, the quality of the electron PID efficiency for the wide path, and also that for the right spectrometer, is identical.

Clean electrons were selected by the gas-cherenkov detector. By electron PID efficiency means what fraction of the clean electron sample the main detector was detecting. The red trace in Fig. 2 shows that this value is close to a unity, which means that the electron PID efficiency was about 100% for this experiment.

Deadtime

Deadtime is the amount of time after each event during which the system is unable to record another event if there is any. Identifying exact value of the deadtime is always a challenge in nuclear physics experiments. To measure deadtime in this experiment, two different resolution times of the electronic modules were used: 30 ns (“narrow path”) and 90 ns (“wide path”). Subsequent events falling within the resolution time of the previous events could not be recorded by the DAQ, causing a counting loss due to deadtime.

A tagger of 10 kHz rate was used to measure the deadtime of the PVDIS electronics. The tagger was mixed with a preshower (P), shower (S), gas-cherenkov (GC) and trigger scintillator (SC) signals separately. After that, these signals were passed through the PVDIS electronics. The output signal from the PVDIS electronics is called PVDIS signal from now on, unless explained otherwise. The PVDIS signal was combined (logical AND) with the tagger itself (see the top sketch in Fig. 3). The idea there was to see if there was any tagger signal killed due to deadtime in PVDIS electronics. After combining a delayed tagger with the tagger-mixed PVDIS signals,

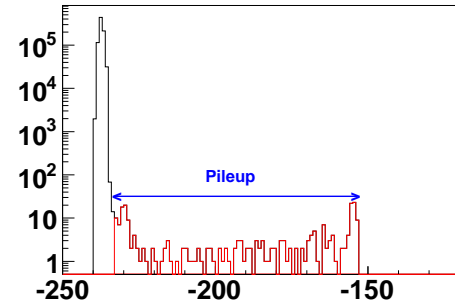
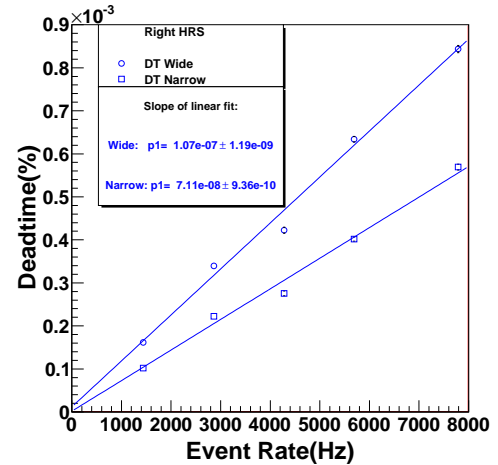
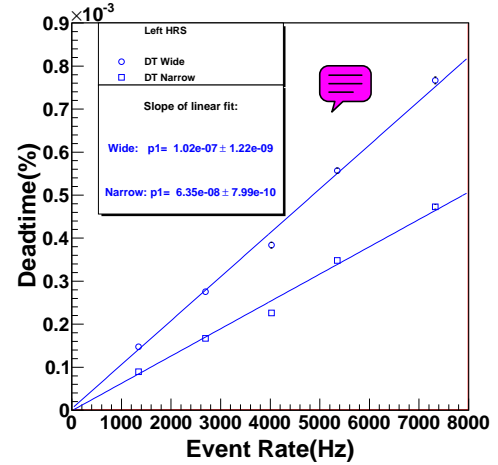
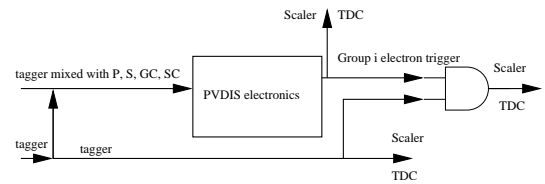


FIG. 3: Top: a diagram for the use of tagger in determining deadtime. Top-second: deadtime plot for a typical group from the left hrs data. Top-third: deadtime plot for a typical group from the right hrs data. Bottom: a TDC plot showing pileup events. The integration of events in the red trace gives the amount of pileup.

we could see the output event rate from the logical AND module to be either equal to the tagger rate itself or less. If the event rate observed from the logical AND output was equal to the tagger rate, there was no deadtime in the PVDIS electronics. If the PVDIS electronics had deadtime, the logical AND output event rate must be smaller than the tagger rate. The fractional loss of tagger event rate is the amount of deadtime (D) which is given as

$$D = 1 - (1 - p)(R_o/R_i),$$

where R_i is the input tagger rate, R_o is the output rate from the logical AND module, and p is a correction factor for pileup effects. The pileup effect arises when the tagger signal follows closely to a PVDIS signal and the DAQ output from the PVDIS electronics coincides with the tagger signal which causes a false count that could have been lost due to the deadtime. The pileup factor p was measured by using the TDC spectrum as shown on the bottom pad in Fig.3. If there was no pileup, only the left-side peak would show up in the TDC spectrum. The integral of the events, other than the left-side peak, would correspond to the pileup amount. Such pileup events are represented by the red trace in the bottom pad in Fig.3.

The slope of deadtime versus rate plot gives the amount of deadtime. This is obtained from the $p1$ -value of each trace in the two middle pads in Fig.3. During the experiment, the narrow path was set as 30 ns and the wide path as 90 ns. The slopes of the left and right hrs wide path traces almost meet the expectation (~ 90 ns) at this early stage of data analysis, and the deadtime of the pvd is electronics appears to be below 1% for any group in the main detector. The similar description for the narrow path, however, does not seem to be possible. The slopes for the narrow paths appear to be around 63 to 71 ns for most of the groups. The reason for that could be due to the input pulses to the pvd is electronics being about 63 to 71 ns. If so, the 30 ns path setting was ineffective. This requires more investigation. Finding the net deadtime of the whole PVDIS electronics and the simulation for the deadtime are the next jobs to be completed.

Asymmetry

The asymmetry is a popular observable that all parity violating experiments care about measuring. Other extractions are possible once the asymmetry is precisely measured. The physics asymmetry sought for in this experiment is about 100 times the Q^2 value. Though the main goal of the present experiment is to extract an effective coupling constant combination ($2C_{2u} - C_{2d}$) with a high precision, it's too early to make any comments on this at the moment, since the data analysis is ongoing. However, for the asymmetry measurements, the following figures (Fig. 4) depict the blinded asymmetry found

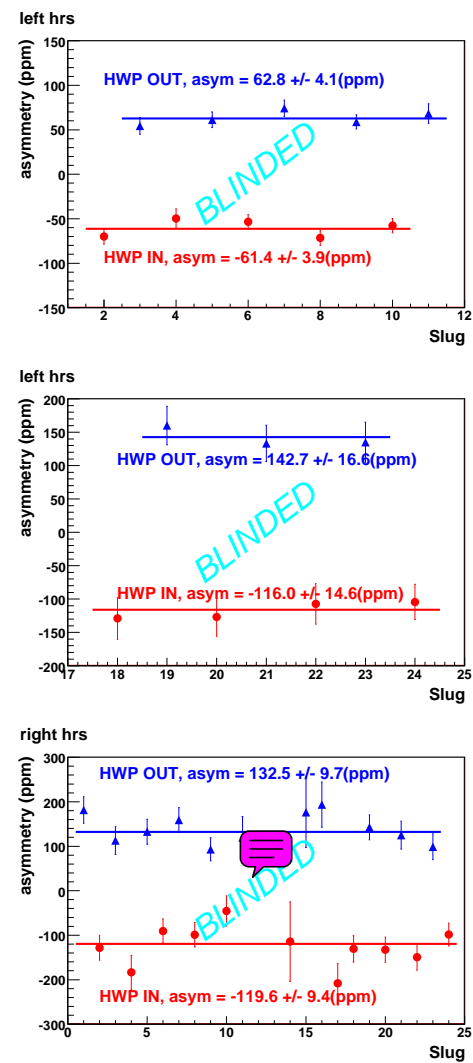


FIG. 4: Asymmetry results during the data taking period. The top plot is from lhs data at low Q^2 ($= 1.1 \text{ GeV}^2/c^2$), middle one is the same at high Q^2 ($= 1.9 \text{ GeV}^2/c^2$), and the bottom plot is from rhs data at high Q^2 ($= 1.9 \text{ GeV}^2/c^2$) again. Any point in a Slug has a data amount of about a day of data taking.

during the time of online analysis. These plots indicate that the quality of data obtained through the counting DAQ meets expectations: asymmetry flips sign with the flipping of spin of the incoming electron beam (i.e., the opposite signs of asymmetries with the half wave plate IN and OUT states), asymmetry increases with the increase of Q^2 value and vice-versa.

Conclusion

The newly developed counting DAQ was successfully implemented in the PVDIS experiment at 6 GeV at Jefferson Lab. The preliminary analysis of deadtime data

indicates that the deadtime of the pvdís electronics is below 1%. The preliminary (blinded) physics asymmetry is meaningful. The overall data analysis of the experiment is progressing.

Jefferson Lab Hall A Proposal E08-011.

[1] R. Michaels, P. Reimer, and X. Zheng, *$\vec{e}^{-2}H$ Parity Violating Deep Inelastic Scattering at CEBAF at 6 GeV,*

[2] X. Zheng, *Parity Violation in Deep Inelastic Scattering at JLab 6 GeV, in PAVI 2006 May 16-20: From Parity Violation to Hadronic Structure and more... (Part III)* (Springer, Milos, Greece, 2006).

[3] R. Subedi et al., AIP proceedings of the 18th International Spin Physics Symposium, 245 (2009).

[4] K. S. Kumar, *Eur. Phys. J. A*, , 191-195 (2005).

[5] J. Alcorn et al., *Nucl. Instr. and Meth.*, , 294 (2004).